Modeling of Dry Ice Accretion on Cylinders – A Case Study of Present Analytical State

Pavlo Sokolov[1], Muhammad S.Virk[1]

[1] *Arctic Technology & Icing Research Group, Institute of Industrial Technology, UiT – The Arctic University of Norway*

pavlo.sokolov@uit.no, muhammad.s.virk@uit.no

Abstract– **The present aggregated knowledge on the atmospheric icing of structures is covered under the framework of the ISO 12494 [1] standard "*Atmospheric Icing on Structures*". When it comes to the ice growth and in particular – the droplet impingement on structural objects, the ISO model is well validated for the rotating cylinders of up to 76 mm in diameter based on experiments of Makkonen and Stallabrass [2] and/or operating conditions which result in the value of the droplet inertia parameter $K > 0.25$ [3]. Recently, Makkonen et al., 2018 [4] have recalculated the droplet trajectories using CFD approach for the values of $0.01 \leq K < 0.25$. Their results show good agreement between the theory and experimental values; however, this does not answer the question of analytical modeling of icing for larger cylinders fully. This work compares two approaches of the analytical modeling with possible application towards the modeling of icing on large conductors – the "spectrum-averaged" calculations using the full droplet distribution spectrum when compared to the Volume Weighted Diameter (VWD) approximation recently proposed by Zhang et al. [5]. The obtained results show that for the value of $K > 0.5$ both approaches tend to be in good agreement with each other and the experimental results, however, for the very high values of $K > 1.5$, the behavior of VWD approximation does not change as with the spectrum-averaged values. For the range of $0.3 < K < 0.5$, the agreement between spectrum-averaged results and the VWD approximation is somewhat worse and depends, in large, on the source distribution(s) used, with wider distributions producing worse agreement. Finally, for the values of $0.25 < K$, the VWD approximation produces significantly lower values of the overall collision efficiencies, albeit, still higher than the MVD approximation, which can potentially be detrimental in designing for and estimating icing loads in such conditions.**

Keywords– ***ice accretion; cylinder; collision efficiency; droplet distribution spectrum; MVD; VWD.***

I. INTRODUCTION

The study of in-cloud icing is not a new scientific field with significant amount of theoretical knowledge regarding modeling of the atmospheric ice accretion accumulated over several dozen years. At present, this aggregated knowledge is incorporated in the governing standard of atmospheric icing modeling the ISO 12494 "*Atmospheric Icing of Structures*" [1]. The theoretical modeling core of it is the Finstad et al. [3] collision efficiency parameterization, which relies on the concept of the so-called "Median Volume Diameter approximation" (MVD) in order to parameterize the in-cloud droplet spectrum using a singular value with the assumption that the cloud droplet distribution can be adequately represented using a uniform droplet distribution, where all the droplets have the same diameter, corresponding to cloud MVD. The initial verification of the concept was carried out by Finstad in the doctoral thesis [6], later expanded in [3], and based on the results of experimental verification of Finstad et al. model by Makkonen and Stallabrass [2] it can be stated that the Finstad et al. model is applicable for the ranges of droplets overall collision efficiencies of $0.07 < E < 0.63$.

However, there are a few potential limitations when it comes to the MVD approximation. First, as noted in [3] the results with MVD approximation tend to underestimate the overall collision efficiencies in cases where the droplet inertia parameter $K < 0.25$. Second, the ISO 12494 also states that the Finstad et al. parameterization tends to underestimate the overall collision efficiencies if $E < 0.10$. Finally, Jones et al. [7] have showed that MVD approximation may not always be valid and in natural conditions, such as on Mt. Washington Observatory, the use of a droplet distribution spectrum can yield significantly better results over a monodisperse distribution when comparing ice accretion data on a multicylinder device.

Recently, it was shown [4] that modern Computational Fluid Dynamics (CFD) tools can achieve good results in modeling of ice accretion on cylinders for cases when $E < 0.10$, granted full droplet distribution spectrum with the "history term" is used. This term (also known as the Basset force) describes the vorticity diffusion from accelerating droplets' surface and the induced mass increase of the droplet due to accelerating air in immediate surroundings are important factors of non-steady state drag term, and term is defined as [6]:

$$F = -\frac{18\rho_f}{\left(2\rho_p + \rho_f\right) d}\left(\frac{\mu}{\pi\rho_f}\right)^{\frac{1}{2}} \int_{-\infty}^{t} \frac{\mathrm{d}u(\tau)}{\mathrm{d}\tau} \frac{\mathrm{d}\tau}{\sqrt{t-\tau}} \qquad (1)$$

where d is the particle diameter, ρ_p and ρ_f are particle and fluid densities, respectively, and $u(\tau)$ is droplet's absolute velocity. As it can be seen from the structure of this term, its singular under integration, and thus is not being possible to solve for "directly", necessitating the usage of certain approximations, such as so-called "window methods" in order to obtain the non-singular closure to it. The question of good approximation of the Basset force is an open problem in fluid dynamics for several decades, which became more popular with increase in widespread usage in CFD tools and availability of computational resources.

The issue of the Basset force is of a certain complexity when it comes to the numerical modeling, however, the complexity is magnified in scope when it comes to the analytical modeling. Thus, the question is, what to do if analytical modeling of icing is required for cases where the overall collision efficiency is expected to be low?

Recently, Zhang et al. [5] have proposed the usage of so-called "Volume Weighted Diameter" approximation, as more

"stable" parameter than MVD, in addition alleviating some of the issue of the underestimating the overall collision efficiencies for low K values. Moreover, Finstad et al. recommends to use a full droplet distribution spectrum for $K < 0.25$. Comparing these two approaches thus will be the main focus of this paper.

II. Design of the Experiment

For the benchmark for comparison, several experimental cases of Makkonen and Stallabrass [2] have been selected. The experiments of Makkonen and Stallabrass were conducted at Low Temperature Laboratory, National Research Council of Canada. The experiments employed a single atomizing spray nozzle at the centerline of 30.5 cm × 30.5 cm test section. Due to expected tunnel blockage effects for some test cases, plenum chambers with perforated walls were installed in place of test section floor and ceiling in order to achieve porosity of test section of 10%. Icing tests were made on horizontally mounted rotating cylinders of 1.024, 3.183, 4.440 and 7.609 cm in diameter. The speed of rotation was 2 RPM.

A water micromanometer was used to measure the dynamic pressure in the tunnel test section. The total temperature of the tunnel air was controlled and measured by a thermostat. The static temperature in the test section (as listed in Table 2 in [2]) was lower than the total temperature, due to the adiabatic expansion of the air accelerating within the contraction. LWC was measured using the single rotating cylinder method while droplet size measurements were done with the Forward Scattering Spectrometer Probe (FSSP). Measurements of the droplet size distributions (listed in the Table 2 in [2]) as "droplet size distribution category") were made at four wind velocities and nozzle settings. More information about experimental setup is available in the original source [2] while the test matrix for this study is given in Table I.

Unfortunately, due to the passage of time the information on droplet distributions in those experiments is no longer available, based on personal communication by Makkonen, so it is not possible to recalculate the results with full distribution spectrum for those experiments, in order to directly compare the results, however, several "synthesized" distributions will be used instead for this work.

Out of all 33 experimental cases, only the cases with highest values of MVD and LWC were selected, as to give the biggest expected ice accretion thickness. To compensate, additional cylinder diameters of 80 – 298 mm have been added for use in further modeling, as to simulate the effect of ice accretion on larger structures and/or for the low values of K. As it is shown in [2] they have utilized a variety of different icing durations in their experiments. However, for this work a "common denominator" of 30 min. icing duration has been used in order to somewhat streamline the comparison. It is expected that this alteration would not skew the values of the overall collision efficiencies by much.

TABLE I. OPERATING CONDITIONS.

Parameter	Value
Cylinder diameter (mm)	10.24, 20, 30, 50, 76.09, 80, 100, 149.5, 170, 249, 298
Cylinder length (m)	0.1
Air velocity (m/s)	20
Air temperature (°C)	–4.5
Icing duration (min)	30
LWC (g/m^3)	0.36
MWD (μm)	17.1
Rotational speed (RPM)	2

In order to study the effect of droplet distribution on the ice accretion process different parameterizations of the droplet spectrum, namely the gamma distributions (also referred as Langmuir distributions) are used [8]. The gamma distributions used in this study are given in Table II in terms of diameter ratios. All gamma distributions have MVD of 17.1 with 'distribution A' being monodispersed. These droplet distributions progressively get "wider" as the ratio of diameters increases, meaning that for distributions with higher value of diameter ratios, the diameters of bins will become progressively smaller or larger, when compared with "preceding" distribution. For the droplet spectrum, each bin collision efficiency is calculated independently and then weighted using the LWC fraction, in order to obtain the overall collision efficiency of the entire spectrum.

The Langmuir distributions B–E were initially presented in [9] as a mathematical approximations of the droplet distribution spectra in fog and rising clouds on Mt. Washington observatory. Later, Howe [8] has presented "wider" droplet distributions F–J, based on previous observations on Mt. Washington observatory, in order to adequately capture bimodal and trimodal droplet distributions, which are expected to happen in nature.

A. Analytical Model

The cloud impingement parameters are calculated in accordance with [3] as:

$$\mathrm{X}(K,\phi) = \left[C_{X,1}K^{C_{X,2}}\exp\left(C_{X,3}K^{C_{X,4}}\right) + C_{X,5}\right] - \\ -\left[C_{X,6}(\phi - 100)^{C_{X,7}}\right] \times \left[C_{X,8}K^{C_{X,9}}\exp\left(C_{X,10}K^{C_{X,11}}\right) + C_{X,12}\right] \quad (2)$$

where X is the cloud impingement parameter of interest, in this particular case the overall collision efficiency E. The constants $C_{X,n}$ are given in [3].

TABLE II. LANGMUIR DISTRIBUTIONS.

LWC fraction	A	B	C	D	E	F	G	H	J
0.05	1.00	0.56	0.42	0.31	0.23	0.18	0.13	0.10	0.06
0.1	1.00	0.72	0.61	0.52	0.44	0.37	0.32	0.27	0.19
0.2	1.00	0.84	0.77	0.71	0.65	0.59	0.54	0.50	0.42
0.3	1.00	1.00	1.00	1.00	1.00	1.00	1.00	1.00	1.00
0.2	1.00	1.17	1.26	1.37	1.48	1.60	1.73	1.88	2.20
0.1	1.00	1.32	1.51	1.74	2.00	2.30	2.64	3.03	4.00
0.05	1.00	1.49	1.81	2.22	2.71	3.31	4.04	4.93	7.34

For the analytical calculations, suing the full droplet distribution spectrum, the "spectrum-averaging" procedure is employed, which is given as:

$$X(K, \phi)_{spec} = \sum w_i X(K_i, \phi)_i \quad (3)$$

where w_i is fractional weight of bin i, subscript i refers to a given parameter calculated for bin i, while subscript *spec* shows spectrum averaged values. The spectrum values are linearly dependent on the per-bin values, as spectrum values, $X(K, \varphi)_{spec}$ are obtained by summation of per-bin values $X(K_i, \varphi)_i$ using LWC fraction w_i as a weighting constant. In addition, the constraint of $X(K_i, \varphi)_i = 0.01$ for $K_i \leq 0.17$ is used as per [3]. Conversely, the VWD is calculated as [5]:

$$\text{VWD} = \sum w_i d_i \quad (4)$$

where d_i is the MVD value of bin i of the droplet distribution spectrum. The VWD approach despite looking similarly to the spectrum-averaging procedure in eq. (3) works a bit differently. The VWD approach first calculates the actual VWD value itself from the distribution, for example, the distributions in Table II, and then estimates the overall collision efficiency from eq. (3) in one iteration, unlike the spectrum-averaging procedure which estimates the overall collision efficiency of each bin of the distribution separately and then sums up the results. However, as evidenced by the structure of the VWD term, the VWD value of the distribution will differ from that of MVD, with Table III giving the VWD values of distributions from Table II, all of which have the MVD value of 17.1 μm.

The ice deposit diameter D_i of cylinder is calculated as [10]:

$$D_i = \left[\frac{4(M_i - M_{i-1})}{\pi \rho_i} + D_{i-1}^2\right]^{1/2} \quad (5)$$

where M is the mass accretion value per unit length, ρ is the ice density and subscript i indicates the time step. In all analytical calculations the time step used is, t = 30 seconds. This is to ensure that the cylinder rotates at least 360° degrees along its longitudinal axis on each time step to ensure even ice deposit on the surface, in accordance with [10]. The accreted ice density at any given time step is calculated as [10]:

$$\rho_i = 378 + 425 \log_{10}(R_m) - 82.3\left(\log_{10}(R_m)\right)^2 \quad (6)$$

where, R_m is the Macklin density parameter, given as:

$$R_m = -\frac{V_0 d}{2 t_s} \quad (7)$$

where d is the MVD in microns, V_0 is the impact velocity of the droplet in m/s and t_s is the surface temperature of the ice deposit in Celsius. In the case of dry growth, the surface temperature of the ice deposit can be obtained as [10]:

$$\frac{2}{\pi} E v w \left(L_f + c_w t_a - c_i t_s\right) = h\left[(t_s - t_a) + \frac{k L_s}{c_p p_a}(e_s - e_a) - \frac{r v^2}{2 c_p}\right] + \sigma \alpha (t_s - t_a) \quad (8)$$

where L_f and L_s are latent heats of fusion and sublimation respectively, c_w, c_i, and c_p are specific heats of water, ice and air respectively, p_a, e_s and e_a are air pressure, saturation water vapour pressures at surface and air temperatures respectively, h is the overall heat transfer coefficient, k = 0.62, r is the recovery factor, with value of 0.79 being used for cylinder, t_s and t_a are surface and air temperatures in Celsius, σ is the Stefan-Boltzmann constant and $\alpha = 8.1 \times 10^7$ K^3. More details on the terms of heat transfer and derivation of heat transfer equations are given in [10].

B. Numerical Setup

The multiphase CFD based numerical simulations were carried out using ANSYS FENSAP-ICE, which uses an Eulerian water droplet impingement solver. The general Eulerian two-phase model for viscous flow consists of the Navier-Stokes equations augmented by the droplets continuity and momentum equations [11]:

$$\frac{\partial \alpha}{\partial t} + \vec{\nabla} \cdot \left(\alpha \overrightarrow{V_d}\right) = 0 \quad (9)$$

$$\frac{\partial \left(\alpha \overrightarrow{V_d}\right)}{\partial t} + \vec{\nabla}\left[\alpha \overrightarrow{V_d} \otimes \overrightarrow{V_d}\right] = = \frac{C_D Re_d}{24K} \alpha \left(\overrightarrow{V_a} - \overrightarrow{V_d}\right) + \alpha \left(1 - \frac{\rho_a}{\rho_d}\right) \frac{1}{Fr^2} \quad (10)$$

where the variables α and $V_{d,a}$ are mean field values of, respectively, the water volume fraction and droplet velocity. The first term on the right-hand-side of the momentum equation represents the drag acting on droplets of mean diameter d. It is proportional to the relative droplet velocity, its drag coefficient C_D and the droplet Reynolds number [11]:

$$Re_d = \frac{\rho_a d V_{a,\infty} \left\| \overrightarrow{V_a} - \overrightarrow{V_d} \right\|}{\mu_a} \quad (11)$$

$$K = \frac{\rho_d d^2 V_{a,\infty}}{18 L_\infty \mu_a} \quad (12)$$

where L_∞ is the characteristic length of the object. In case of the cylinder, the characteristic length is cylinder radius. The second term represents buoyancy and gravity forces, and is proportional to the local Froude number [11]:

$$\text{Fr} = \frac{\left\| V_{a,\infty} \right\|}{\sqrt{L_\infty g_\infty}} \quad (13)$$

These governing equations describe the same physical droplet phenomenon as the Lagrangian particle tracking approach. Only the mathematical form in which these equations are derived changes, using Partial Differential Equations instead of Ordinary Differential Equations. The droplet drag coefficient is based on an empirical correlation for flow around spherical droplets, or [11]:

$$C_D = (24/Re_d)\,(1 + 0.15 Re_d^{0.687}) \quad \text{for} \quad Re_d \leq 1300$$

$$C_D = 0.4 \quad \text{for} \quad Re_d > 1300$$

TABLE III. VWD VALUES FOR DISTRIBUTIONS FROM TABLE II.

Distribution	A	B	C	D	E	F	G	H	J
VWD (μm)	17.10	17.25	17.61	18.27	19.10	20.17	21.52	23.21	27.58

The droplet local collision efficiency is calculated as follows [11]:

$$\beta = -\frac{\alpha \overrightarrow{V_d} \cdot \vec{n}}{(LWC)V_\infty} \tag{14}$$

where α is the local volume fraction (kg/m^3) and $\vec{n}$ is the surface normal vector. The total collision efficiency is an integration of local collision efficiencies over the surface area and is given as [11]:

$$\beta_{tot} = \frac{\int \beta \, dA}{L_\infty^2} \tag{15}$$

The ice density calculation procedures in FENSAP follows that given in the analytical model.

Detailed mesh sensitivity analysis was carried out to accurately determine the boundary layer characteristics (shear stress and heat fluxes), a *y*+ values of less than 1 is used near the cylinder wall surface. Number of mesh elements and *y*+ value was selected based upon the heat flux calculations, where a numerical check was imposed that the heat flux computed with the classical formulae d*t*/d*n* should be comparable with the heat flux computed with the Gresho's method.

III. Results and Discussion

Tables IV and V list the overall collision efficiency values for the Langmuir distributions and the VWD, respectively. The "*Ref*" column shows the values of the experimental overall collision efficiencies from [2], where applicable.

From the Tables IV and V it can be seen that for higher values of the droplet inertia parameter, $K > 0.5$ the VWD approximation tends to yield higher values of the overall collision efficiencies for all tested distributions. Furthermore, observe that for very high value of $K > 1.5$, corresponding to cases of 10.24 and 20 mm cylinders, the Langmuir distributions are giving the smaller values of *E* than the monodisperse distributions. This behavior as was originally noted in [9] who first implemented the distributions B–E. However, since the VWD approximation is a monodisperse distribution, the similar behavior does not apply to it, so the values of the overall collision efficiency will continue to increase with the increase of *K*, in addition, the bigger VWDs have higher value of *K* by default as they are larger diameter droplets.

For the ranges of $0.4 < K < 0.75$, corresponding to the 50–100 mm cylinders both VWD and spectrum-averaged values are in relatively good agreement, with exception of results for wide distributions G–J, for which VWD tends to scale up in values much more "aggressively". In general, the VWD approximation is more sensitive to the change in droplet distribution spectrum than the spectrum-averaging procedure for the higher values of *K*. However, for the cases of 149.5–298 mm cylinders, which corresponds to the value of $K < 0.25$ the situation reverses and the spectrum-averaged results show higher values of overall collision efficiencies and bigger changes arising with the change of distribution.

This can be explained by the fact that in such conditions, the bigger sized droplets within a distribution are a dominating factor when it comes to the values of the overall collision efficiency, due to highly non-linear dependence of it on droplet size, while the smaller droplets contribute less, but still add to the overall collision efficiency due to constraint of $X(K_i, \varphi)_i = 0.01$ for $K_i \leq 0.17$ being enforced. While there is not enough experimental data for validation of both said concepts at very low values of *K*, in general, the usage of spectrum-averaging is a more "safe" choice when it comes to design guidelines, as this method will provide considerably higher ice masses in the theoretical modeling.

TABLE IV. ANALYTICAL VALUES OF OVERALL COLLISION EFFICIENCIES USING LANGMUIR DISTRIBUTIONS.

D (mm)	Mono	Lang B	Lang C	Lang D	Lang E	Lang F	Lang G	Lang H	Lang J	Ref
10.24	0.554	0.541	0.532	0.525	0.518	0.512	0.508	0.505	0.502	0.56
20	0.414	0.405	0.401	0.401	0.402	0.402	0.406	0.411	0.417	–
31.83	0.303	0.298	0.300	0.306	0.312	0.320	0.329	0.338	0.353	0.32
50	0.196	0.197	0.204	0.216	0.229	0.241	0.254	0.268	0.294	–
76.09	0.111	0.117	0.128	0.143	0.158	0.176	0.192	0.209	0.238	0.18
80	0.102	0.109	0.120	0.135	0.151	0.168	0.185	0.202	0.231	–
100	0.067	0.076	0.087	0.104	0.121	0.138	0.155	0.172	0.203	–
149.5	0.022	0.035	0.046	0.060	0.074	0.090	0.107	0.123	0.155	–
170	0.012	0.026	0.036	0.048	0.062	0.077	0.093	0.109	0.141	–
249	0.010	0.013	0.019	0.027	0.038	0.050	0.064	0.078	0.109	–
298	0.010	0.011	0.014	0.020	0.029	0.040	0.052	0.065	0.094	–

TABLE V. ANALYTICAL VALUES OF OVERALL COLLISION EFFICIENCIES USING VWD APPROXIMATION.

D (mm)	Mono	VWD B	VWD C	VWD D	VWD E	WVD F	WVD G	VWD H	WVD J	Ref
10.24	0.554	0.557	0.566	0.581	0.598	0.619	0.644	0.671	0.727	0.56
20	0.414	0.418	0.428	0.445	0.465	0.490	0.518	0.551	0.621	–
31.83	0.303	0.307	0.316	0.334	0.354	0.380	0.411	0.446	0.523	0.32
50	0.196	0.199	0.208	0.224	0.243	0.268	0.297	0.333	0.413	–
76.09	0.111	0.114	0.120	0.133	0.150	0.170	0.196	0.228	0.305	0.18
80	0.102	0.105	0.111	0.124	0.139	0.160	0.185	0.216	0.292	–
100	0.067	0.069	0.075	0.085	0.098	0.116	0.138	0.166	0.236	–
149.5	0.022	0.023	0.027	0.033	0.042	0.054	0.069	0.090	0.145	–
170	0.012	0.013	0.016	0.021	0.029	0.039	0.052	0.070	0.120	–
249	0.010	0.010	0.010	0.010	0.010	0.010	0.015	0.027	0.060	–
298	0.010	0.010	0.010	0.010	0.010	0.010	0.010	0.013	0.039	–

Tables VI and VII present the numerical results in the CFD simulations and the comparison between numerical and analytical results, respectively. However, due to rather significant time expenditures on the CFD simulations, only cases D and E in addition to monodisperse distributions simulations have been performed. The choice of distributions D and E is deemed to be "representative" as they are mostly being "in the middle" as it can be seen from Tables II and III.

TABLE VI. NUMERICAL VALUES OF OVERALL COLLISION EFFICIENCIES IN CFD SIMULATIONS.

D (mm)	Mono	VWD D	VWD E	Lang D	Lang E
10.24	0.562	0.592	0.610	0.533	0.526
20	0.386	0.419	0.439	0.380	0.383
31.83	0.249	0.278	0.296	0.261	0.270
50	0.171	0.199	0.217	0.194	0.208
76.09	0.081	0.101	0.114	0.116	0.116
80	0.082	0.096	0.109	0.117	0.125
100	0.051	0.067	0.079	0.088	0.104
149.5	0.015	0.022	0.028	0.045	0.058
170	0.009	0.015	0.019	0.038	0.051
249	0.003	0.004	0.005	0.017	0.025
298	0.002	0.002	0.003	0.010	0.017

As it can be seen from Tables VI and VII the behavior of both spectrum-averaging and VWD approximations in the CFD simulations is relatively the same as in case with analytical modeling, thus the preceding discussion and its conclusions do apply for numerical modeling also, however, some of the obtained values in CFD when compared to analytical results are somewhat different and thus need explanation.

First, observe that for majority of cases tested the CFD values show lower overall collision efficiencies. This can be explained by the viscous treatment of the flow, as the boundary layer effects are much more prominent and do influence smaller droplet's "pushing" them "away" from the cylinder into the flow's streamline. This effect becomes more significant with the increase of cylinder's diameter as it can be inferred from the results for the monodispersed case. Second, observe significantly lower values for the larger cylinder diameters, in particular 249 and 298 mm one in the CFD simulations. The reason for this is that the constraint of $X(K_i, \varphi)_i = 0.01$ for $K_i \leq 0.17$ is not employed in the numerical simulations, thus the overall collision efficiency can be an arbitrary small positive value much less than 0.01. Therefore, based on these results, the CFD modeling can be used for both the spectrum-averaging and the VWD approximation approaches, and as with the VWD approach itself, the best results are reached for the cases with $K > 0.5$. Finally, the results from Table VII are given in graphical form in Fig. 1 for the ease of quick comparison.

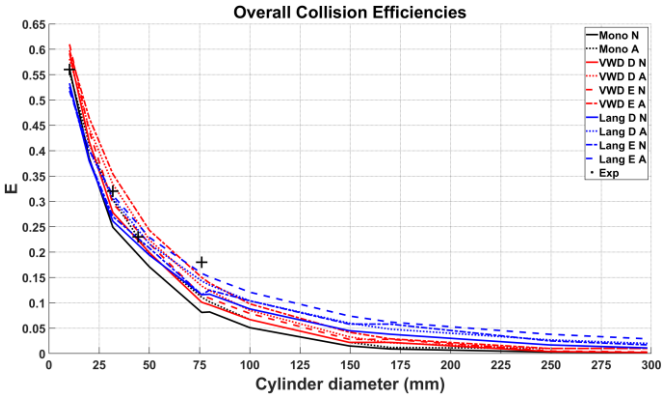

Fig.1. Overall collision efficiencies for the cases from Table VII. The black crosses represent experimental values from the (Makkonen and Stallabrass, 1987) experiments. Letters "*A*" and "*N*" indicate the analytical and the numerical results, respectively.

IV. CONCLUSION

In this work the detailed comparison between the "spectrum-averaging" procedure and the Volume Weighted Diameter (VWD) has been performed for the wide range of cylinder diameters in order to test the applicability and performance of both concepts over a wide range of values of the droplet inertia parameter *K*. The results show that for the value of $K > 0.5$ both approaches tend to be in good agreement with each other and the experimental results, however, for the very high values of $K > 1.5$, the behavior of VWD approximation does not change as with the spectrum-averaged values. In general, for $K > 0.5$ the VWD approximation is very sensitive towards the source distribution(s). For the range of $0.3 < K < 0.5$, the agreement between spectrum-averaged results and the VWD approximation is somewhat worse and depends, in large, on the source distribution(s) used, with wider distributions producing worse agreement. Finally, for the values of $0.25 < K$, the VWD approximation produces significantly lower values of the overall collision efficiencies, albeit, still higher than the MVD approximation, which can potentially be detrimental in designing for and estimating icing loads in such conditions, such as, long-term accretion of power lines, power line and communication towers etc.

Fundamentally, while VWD approximation does alleviate some issues of the MVD approximation, for low values of *K*, such as $0.25 < K$, it does not achieve much added performance

TABLE VII. COMPARISON OF OVERALL COLLISION EFFICIENCIES ACROSS THE MODELS.

D (mm)	Mono Num	Mono Ana	VWD D Num	VWD D Ana	VWD E Num	VWD E Ana	Lang D Num	Lang D Ana	Lang E Num	Lang E Ana
10.24	0.562	0.554	0.592	0.581	0.61	0.598	0.533	0.525	0.526	0.518
20	0.386	0.414	0.419	0.445	0.439	0.465	0.380	0.401	0.383	0.402
31.83	0.249	0.303	0.278	0.334	0.296	0.354	0.261	0.306	0.270	0.312
50	0.171	0.196	0.199	0.224	0.217	0.243	0.194	0.216	0.208	0.229
76.09	0.081	0.111	0.101	0.133	0.114	0.150	0.116	0.143	0.116	0.158
80	0.082	0.102	0.096	0.124	0.109	0.139	0.117	0.135	0.125	0.151
100	0.051	0.067	0.067	0.085	0.079	0.098	0.088	0.104	0.104	0.121
149.5	0.015	0.022	0.022	0.033	0.028	0.042	0.045	0.060	0.058	0.074
170	0.009	0.012	0.022	0.021	0.028	0.029	0.038	0.048	0.058	0.062
249	0.003	0.010	0.004	0.010	0.005	0.010	0.017	0.027	0.025	0.038
298	0.002	0.010	0.002	0.010	0.003	0.010	0.011	0.020	0.017	0.029

when it comes to estimating the overall collision efficiencies, while, simultaneously, for very high values of K it can overestimate the overall collision efficiency. Ultimately, its lesser complexity when compared to the spectrum-averaging does not warrant the use in these sort of conditions, while for higher values of K, i.e., $0.3 < K < 0.7$ its usage may be warranted over the MVD approximation to produce higher estimates of the overall collision efficiency.

ACKNOWLEDGEMENT

The work reported in this paper is funded by the Research Council of Norway, IceBOX- project no 282403.

REFERENCES

[1] ISO 12494:2001(E), 2001. *Atmospheric icing of structures*. Standard. International Organization for Standardization. Geneva, CH

[2] Makkonen, L., Stallabrass, J.R., 1987. *Experiments on the cloud droplet collision efficiency of cylinders*. Journal of Applied Meteorology 26, 1406-1411.doi:10.1175/1520-0450(1987)026<1406:EOTCDC>2.0.CO;2

[3] Finstad, K.J., Lozowski, E.P., Gates, E.M., 1988. *A computational investigation of water droplet trajectories*. Journal of Atmospheric and Oceanic Technology, 5, 160-170.doi:10.1175/1520-0426(1988)005<0160:ACIOWD>2.0.CO;2

[4] Makkonen, L., Zhang, J., Karlsson, T., Tiihonen, M., *Modelling the growth of large rime ice accretions*, CRST, 151 (2018), 133-137.

[5] Zhang, J., Qing, H., Makkonen, L., *A novel water droplet size parameter for calculation of icing on power lines*. Coltec (2017) https://doi.org/10.1016/j.coldregions.2018.01.021, pre-print

[6] Finstad, K. J. 1986. *Numerical and experimental studies of rime ice accretion on cylinders and airfoils*. Ph.D. thesis. University of Alberta, Canada.doi:10.7939/R3N58CS1V.

[7] Jones, K.F., Thompson, G., Claffey, K.J., Kelsey, E.P, 2014, *Gamma Distribution Parameters for Cloud Drop Distributions from Multicylinder Measurements*. Journal of Applied Meteorology and Climatology, vol. 53, pp. 1606 – 1617. doi: 10.1175/JAMC-D-13-0306.1

[8] Howe, J.B. 1990. *The rotating multicylinder method for the measurement of cloud liquid water content and droplet size*. CRREL Report.

[9] Langmuir, I., Blodgett, K., 1946. *A Mathematical Investigation of Water Droplet Trajectories*. Army Air Forces technical report 5418. Army Air Forces Headquarters, Air Technical Service Command.

[10] Makkonen, L., 1984. *Modeling of Ice Accretion on Wires*. Journal of Applied Meteorology 23, 929-939. doi:10.1175/1520-0450(1984)023<0929:MOIAOW>2.0.CO;2

[11] FENSAP–ICE User Manual